sustainability

MDPI

Article

Experimental Investigation of Low-Carbon Concrete Using Biochar as Partial Cement Replacement

Ali A. Abbas * and Sagar J. Thapa

Department of Engineering and Construction, School of Architecture, Computing and Engineering, University of East London, Docklands Campus, London E16 2RD, UK

* Correspondence: abbas@uel.ac.uk

Abstract

Cement is the primary binder in concrete and a major contributor to global CO_2 emissions. This experimental study investigates the use of biochar as a partial replacement for cement to develop low-carbon concrete. Material characterisation included particle size distribution, density, and water absorption of biochar and aggregates, followed by tests on setting time, workability, compressive strength, and dry density. The embodied carbon of each mix was also calculated to evaluate the reduction in emissions. Six mixes were produced with 0%, 5%, 15%, 30%, 45%, and 60% biochar replacement by weight of CEM I. Results indicated that biochar has high water absorption and low specific gravity, which reduced workability and strength at higher replacement levels, but significantly decreased the embodied carbon. The findings suggest biochar's potential use in non-structural, low-strength concrete applications such as concrete blocks.

Keywords: biochar; low-carbon concrete; carbon sequestering; concrete structures; compressive strength; embodied carbon

check for updates

Academic Editors: Antonio Caggiano and Hosam Saleh

Received: 29 September 2025
Revised: 17 November 2025
Accepted: 27 November 2025
Published: 1 December 2025

Citation: Abbas, A.A.; Thapa, S.J. Experimental Investigation of Low-Carbon Concrete Using Biochar as Partial Cement Replacement. *Sustainability* **2025**, *17*, 10744. https://doi.org/10.3390/su172310744

1. Introduction

1.1. Background

Anthropogenic CO_2 emissions are one of the major causes of global warming, posing a serious threat to ecosystems and the built environment [1]. Among all construction materials, concrete is the most widely used after water and represents a significant source of CO_2 emissions due to its main component, cement. Cement manufacturing alone accounts for approximately 7–8% of global CO_2 emissions. In response, governments, including the UK, have committed to achieving net-zero emissions by 2050 [2]. To address these environmental challenges, research has increasingly focused on developing low-carbon concrete by partially replacing cement with Supplementary Materials such as fly ash, ground granulated blast-furnace slag (GGBS), and other industrial by-products. More recently, biochar, a carbon-rich by-product of biomass pyrolysis, has gained attention as a sustainable and carbon-sequestering material for concrete [3]. Biochar not only has the potential to store carbon but also to modify concrete properties due to its high porosity and surface area. However, despite promising findings, biochar's variable characteristics, depending on feedstock type and pyrolysis conditions, make it challenging to develop a standardised mixed design or predict consistent performance outcomes. Furthermore, while several studies have explored biochar's physical and mechanical effects, few have simultaneously examined its influence on the embodied carbon of concrete.

Therefore, the present experimental study aims to evaluate the fresh, hardened, and environmental performance of concrete incorporating biochar as a partial cement replacement. This research contributes to the existing knowledge by linking mechanical behavior and embodied carbon assessment, providing insight into biochar's suitability for low-carbon, non-structural concrete applications.

1.2. Research Objectives

The main objective of the present experimental study is to experimentally evaluate the potential of biochar as a partial replacement for cement in low-carbon concrete. Specifically, the research aims to:

- Characterise the physical properties of biochar and aggregates, including particle size, water absorption, and density.
- Develop and test concrete mixes incorporating different biochar replacement levels (0%, 5%, 15%, 30%, 45%, and 60%) and compare them with a control mix.
- Examine the fresh properties (workability and setting time) and hardened properties (compressive strength and dry density) of the mixes.
- Estimate the embodied carbon of each mix and assess the overall potential for carbon footprint reduction in biochar concrete.

1.3. Literature Review

The literature review summarised below provides an overview of biochar production methods and key characteristics, while also examining how biochar impacts the properties of both fresh and hardened concrete.

1.3.1. Biochar Production and Its Properties

When biomass and organic matter such as wood, grass, or vegetable waste are pyrolyzed, a carbon-rich solid known as biochar is produced. During pyrolysis, three by-products are generated: solid, liquid, and gaseous components. The solid fraction biochar is typically black in colour, rich in carbon, and possesses strong carbon-capturing capacity.

In the pyrolysis process, the feedstock is subjected to high temperatures (generally above 400 °C) under limited oxygen conditions, which alters its internal structure and significantly increases its surface area and porosity compared to the original biomass [4]. As heating progresses, hydrogen and volatile carbon compounds are released, leaving behind an aromatic carbon residue [4,5]. The feedstock thus undergoes thermal decomposition, forming syngas (gaseous phase), bio-oil (liquid phase), and solid char (biochar). The proportions of these products vary with pyrolysis conditions, such as temperature, residence time, and heating rate [6]. The internal structure and physical properties of biochar depend strongly on the quality and type of biomass used. According to Downie et al. [7], while the size and mass of the biomass change during pyrolysis, the mineralogical composition and porosity of biochar remain largely stable. Biochar quality is influenced by pre-treatment (drying, crushing), processing conditions (heating rate, duration, temperature), and post-processing (grinding).

Among these factors, the highest treatment temperature (HTT) is generally considered the most influential parameter controlling porosity, surface area, and carbon yield [7–9]. For instance, Lua et al. [8] found that biochar samples produced at higher temperatures exhibited improved porosity and surface area. Increasing HTT has been shown to increase porosity, carbon content, and reduce volatile matter [9,10]. The physical characteristics of biochar vary according to both the biomass source and pyrolysis temperature. A summary of representative findings from the literature is presented in Table 1, which illustrates how

properties such as relative density, carbon content, and absorption capacity change with feedstock type and temperature [10,11].

Table 1. Physical properties of biochar for different types of biomasses and pyrolysis conditions.

Reference	Biomass	Temperature	Size of Particles	Relative Density	Carbon Percentage	Absorption Capacity
[10]	Biochar as Wood sawdust	300 °C	3–200 Micrometer	1.59	62.3%	736%
		500 °C		1.51	87.2%	879%
[11]	Biochar as a Paper sludge	500 °C	Not available	Not available	30.0%	Not available
[12]	Biochar as Wood sawdust	300 °C	3 to 200 Micrometer	1.54	68.3%	246%

1.3.2. Impact of Biochar on Cement Hydration

The addition or partial replacement of cement with Supplementary Materials such as fly ash, GGBS, or biochar can influence the rate and mechanism of cement hydration. Both physical and chemical factors play significant roles in this process [13]. Chemically, pozzolanic reactions involve the reaction of amorphous siliceous and alumina-based compounds with calcium hydroxide (released during cement hydration) and water to form additional calcium silicate hydrate (C–S–H) and calcium aluminate hydrate (C–A–H) gels. Biochar generally contains a very low silica content (typically < 0.5 wt %) and therefore is not usually classified as pozzolanic. However, Zeidabadi et al. [14] reported that rice husk and bagasse-based biochars can contain up to 13% silica following pretreatment. Thus, the pozzolanic contribution of biochar depends on its feedstock and production conditions. Biochars with negligible reactive silica behave primarily as fillers, whereas those with higher reactive silica may participate weakly in pozzolanic reactions, forming additional hydration products that refine pore structure.

From a physical perspective, biochar is largely chemically inert, and its influence on microstructure arises from its physical characteristics—a phenomenon commonly termed the filler effect. This mechanism comprises three components: cement dilution, particle-size distribution, and nucleation [15]. Replacing cement with an inert material such as biochar leads to dilution, thereby reducing the total amount of hydration products. However, biochar particles can improve particle packing by filling micro-voids in the cement matrix, while the nucleation effect provides additional sites for hydrate growth, enhancing early hydration kinetics. Biochar's high water absorption capacity also affects hydration. The interfacial transition zone (ITZ) between cement pastes and aggregate strongly influences mechanical and durability performance [16]. The ITZ depends on factors such as particle shape, texture, porosity, and water-retention capacity [17]. Aggregates with higher porosity can enhance mechanical interlock and increase the local degree of hydration by providing additional internal water. This principle can also apply to biochar particles. The ITZ between biochar and cement paste was denser than that between sand and cement paste, attributing this to enhanced hydration through water migration and better mechanical interlocking of hydration products within biochar pores [18]. Applying a biochar coating to polypropylene (PP) fibers enhanced fiber–matrix bonding, reduced micro-air pocket formation, and decreased permeability [12]. The coating roughened fibre surfaces and enabled water retention and delayed release, resulting in denser paste and improved strength.

1.3.3. Impact of Biochar on Properties of Fresh Concrete

Biochar possesses a high-water absorption capacity, attributed to its large surface area and porous internal structure. Reported absorption capacities typically range between 200 and 800% by weight, depending on feedstock type and pyrolysis temperature [9,12]. Due to this property, biochar can absorb part of the mixing water, effectively lowering the free water-to-cement ratio in the concrete mixture. Experimental findings indicate that incorporating biochar reduces workability. For example, Dixit et al. [19] reported a 25% decrease in flow in ultra-high-performance concrete (UHPC) containing 8 wt.% biochar. This reduction in slump is attributed to water absorption and the increased internal friction caused by fine, porous particles. When fine biochar is dispersed in the mix, it can also act as a micro-filler and nucleation site, enhancing hydration kinetics and promoting early strength development [20]. The initial setting time has been found to decrease by 10–25% with biochar additions up to 5 wt.%, indicating accelerated hydration. Biochar: The inclusion of fine biochar increases the matrix density by filling voids between cement and sand grains, which improves cohesiveness and reduces the potential for bleeding.

In summary, the incorporation of biochar into fresh concrete leads to reduced workability, lower effective w/c ratio, and accelerated setting times, with the magnitude of change depending primarily on biochar fineness, porosity, and dosage.

1.3.4. Effect of Biochar on Properties of Hardened Concrete

Quantitatively, the addition of fine biochar typically increases the compressive strength by 3–10% when the replacement level is $\leq$5 wt.%, whereas higher dosages (>10–15 wt.%) tend to reduce strength by 20–40% due to dilution and reduced binding phases [14,19]. Similarly, an increase in fracture energy of approximately 25% and improved electromagnetic shielding properties in mortar containing $\leq$1 wt.% biochar derived from nut shells [21]. Incorporating up to 2 wt.% biochar was found to improve both compressive and tensile strength by enhancing interfacial bonding and decreasing matrix porosity [22]. Overall, incorporating small proportions of biochar ($\leq$5 wt.% of cement) can marginally improve compressive strength, fracture energy, and microstructural density, while excessive replacement levels generally weaken the concrete matrix due to reduced cementitious binding. The summarised quantitative findings of these studies are presented in Table 2.

Table 2. Summary of various applications of biochar in concrete.

Reference	Biochar Type	Application	Biochar Percentage	Major Outcomes
[14]	Biochar from Rice husk	Used as Cement replacement in mortar	Less or equal to 10% weight of cement	The increase in strength by 5% can be attributed to the pozzolanic activity of biochar, while a decrease in strength by 10% may be due to the dilution of cement.
[19]	Biochar from Wood dust	Used in UHPC as partial cement. replacement	Less or equal to 8% by wt. of cement replacement	Hydration level increased; compressive strength decreased by 8–15% for coarser biochar.
[21]	Biochar from Nuts shell	Used as a Supplement/additive in mortar	Less or equal to 1% of the weight of cement	Fracture energy increased by ~25–30% developed concrete with enhanced electromagnetic shielding effectiveness (up to 15 dB improvement).

Table 2. *Cont.*

Reference	Biochar Type	Application	Biochar Percentage	Major Outcomes
[23]	Biochar from Plywood (Eucalyptus)	Used in a previous Concrete as a Cement replacement	Less or equal to 6.5% replacement by wt.	Compressive & splitting tensile strength increased—up to ~33% at 6.5% replacement; porosity/permeability maintained

1.3.5. Effect of Biochar on the Durability of Concrete

Durability in hardened concrete largely depends on its pore structure and permeability. A dense cement matrix with a finely connected pore network improves resistance to moisture and ion ingress, thereby enhancing long-term durability [24,25]. Conversely, a more porous matrix increases the likelihood of deterioration through carbonation, freeze–thaw cycles, and chloride penetration. Electrical conductivity testing provides another means of assessing durability by quantifying the ability of concrete to resist ionic transport under an applied potential. Electrical conductivity testing provides another means of assessing durability by quantifying ionic transport resistance. The measured resistivity depends on factors such as temperature, degree of saturation, pore-solution conductivity, and microstructural connectivity [25]. The inclusion of biochar can influence these parameters by altering pore structure and adding conductive carbonaceous pathways. Because biochar is composed primarily of amorphous and graphitic carbon, several studies have identified it as a moderately conductive material [24,26–28]. High-temperature biochars (600–700 °C) exhibited up to three-fold greater electrical conductivity than those produced below 400 °C, due to higher fixed-carbon content and lower volatile matter [29]. Consequently, biochar incorporation can either increase or decrease the electrical resistivity of concrete depending on dosage and microstructural interaction with the cement matrix.

Overall, low dosages of fine biochar (<3 wt.% cement replacement) can refine pore structure and slightly enhance impermeability, while higher contents tend to increase overall porosity and reduce resistivity, potentially influencing durability performance.

1.3.6. Effect of Biochar on the Internal Curing of Concrete

Internal curing is a well-established concept used to sustain hydration in low water-to-cement (w/c) ratio concretes. Traditionally, it is achieved through lightweight aggregates (LWA) that absorb water during mixing and gradually release it as hydration proceeds [30]. However, biochar—a highly porous, carbon-rich material—can serve a similar or complementary role due to its unique microstructural characteristics. Biochar possesses a highly porous, sponge-like microstructure with a large internal surface area and significant water absorption and retention capacity [7]. These characteristics enable biochar particles to store part of the mixing water and later release it into the cement matrix during hydration, compensating for moisture loss due to self-desiccation or external drying. Compared with conventional LWA, biochar typically exhibits smaller particle sizes (<63 μm) and higher specific surface area, allowing more uniform dispersion throughout the cementitious matrix and a reduced spacing factor, which shortens the path for water migration and improves local hydration [31].

Experimental evidence supports this mechanism. Mrad and Chehab [18] replaced up to 45 wt.% of sand with biochar in mortar and observed that water-cured specimens exhibited a reduction in compressive strength due to biochar's lower mechanical stiffness relative to sand. However, air-cured specimens displayed 15–20% higher retained strength compared to the control, indicating that biochar's internal water release mitigated moisture

loss under limited-curing conditions. Incorporation of 2 wt.% biochar (by weight of cement) improved compressive strength by approximately 8–12% under both dry and pre-soaked conditions, with more pronounced benefits observed during air curing [10]. Therefore, the internal curing effect of biochar arises from its microporous structure, high water-holding capacity, and distributed release of moisture during hydration, which collectively enhance cement hydration and microstructural development, especially in concretes exposed to suboptimal curing environments.

1.3.7. Use of Biochar for Internal Carbonation on Concrete

Carbonation is a physicochemical process in which atmospheric carbon dioxide reacts with calcium hydroxide ($Ca(OH)_2$) in hydrated cement paste to form calcium carbonate ($CaCO_3$). This reaction lowers pore solution alkalinity (pH < 9), increasing the risk of reinforcing-steel corrosion. The incorporation of biochar can influence this process through its high internal surface area, microporosity, and CO_2 adsorption capacity, which enable it to trap and retain carbon dioxide molecules within the cementitious matrix [32]. Experimental results indicate that adding 1–3 wt.% biochar can reduce carbonation depth by 20–35% and lower the chloride diffusion coefficient by approximately 15–25% compared to control specimens [32,33]. These effects are attributed to enhanced pore refinement and CO_2 capture by biochar particles. However, some strength reductions have been observed following carbonation treatment. Mortar specimens containing CO_2-treated biochar exhibited 8–12% lower compressive strength and 10–15% lower tensile strength compared to those with untreated biochar, likely due to microcracking and debonding from local expansion caused by calcium carbonate formation [33]. Similarly, 1 wt.% pre-treated biochar caused moderate reductions in mechanical performance, indicating that while carbonation improves CO_2 sequestration and microstructural densification, it may compromise strength at higher dosages or treatment intensities. Overall, biochar's ability to adsorb and chemically bind CO_2 within concrete contributes to carbon mitigation and microstructural modification. The balance between carbonation-induced densification and strength loss depends on biochar dosage, feedstock, and surface modification conditions.

1.3.8. Use of Biochar on Concrete for Carbon Adsorption

Adsorption is defined as the interaction of two distinct phases, in this case, carbon dioxide and biochar, at the molecular level [34]. This process can occur through physical (van der Waals) or chemical (activated) adsorption. Physical adsorption is governed by intermolecular forces such as van der Waals interactions, typically involve low binding energy, and does not result in significant chemical changes. The adsorption of CO_2 by biochar is generally considered an exothermic process dominated by physical (van der Waals) interactions [35,36]. Experimental studies indicate that increasing pressure can enhance CO_2 adsorption efficiency [34,36]. Key factors affecting biochar's adsorption capacity include its specific surface area and pore size distribution [37]. Several studies have demonstrated that biochar produced at higher pyrolysis temperatures exhibits higher CO_2 adsorption capacities [9,35,38].

1.3.9. Application of Biochar to Develop Low-Carbon Concrete

Incorporating biochar at 10 wt.% was reported to significantly reduce overall CO_2 emissions based on life cycle assessment results. Biochar blocks containing 30 wt.% biochar in combination with supplementary cementitious materials (SCMs) were shown to achieve a carbon-negative status by sequestering 59–65 kg CO_2 per tonne [39]. The CO_2 reduction relative to biochar content indicates a strong potential for enhancing carbon sequestration in biochar-based concrete [40]. Processing biochar with 4 wt.% stearic acid ($C_{17}H_{35}CO_2H$) in a planetary ball mill for three hours produced a super-hydrophobic carbonaceous

powder, which, when used to replace 15% of Portland cement, lowered the embodied carbon footprint by approximately 45% compared to the control mix [41]. Additionally, 5% replacement of cement with biochar could sequester 32.4 kg CO_2/m^3, while the biochar treatment further reduced greenhouse gas emissions by 15.8 kg CO_2/m^3 [39].

1.3.10. Summary

The literature demonstrates that biochar influences hydration, workability, strength, and durability primarily through physical mechanisms rather than pozzolanic activity. Its effects depend on feedstock, particle size, and pyrolysis conditions. At low dosages, biochar enhances water retention, internal curing, and hydration; excessive replacement, however, weakens strength and workability. Most prior work investigated $\leq$ 10% replacement, leaving the behaviour at higher levels insufficiently understood. The present study, therefore, explores a wider replacement range (5–60%) to quantify both mechanical and carbon-reduction performance, offering a broader experimental foundation for sustainable low-carbon concrete design.

2. Methodology

2.1. Introduction

This section outlines the experimental procedure, including material selection, sampling, characterisation, mix design, casting, testing, and analysis of both fresh and hardened concrete properties. All tests were performed following British Standards and established laboratory procedures. A comprehensive understanding of material characteristics is essential in civil engineering research. This experimental approach aimed at evaluating biochar as a sustainable, low-carbon replacement for cement, supporting the global objective of carbon-neutral construction

2.2. Materials and Their Characterisation Test

Cement, natural aggregates, and biochar were the primary materials used in this study. The biochar was a commercially available soil-grade product derived from hardwood biomass through medium-temperature pyrolysis (approximately 450–550 °C) under low-oxygen conditions, in accordance with the European Biochar Certificate (EBC) standards [42]. The resulting material was carbon-rich, highly porous, and slightly alkaline (pH $\approx$ 8.5–10), with a bulk density of 1.2–1.6 g/cm^3 and a fine particle size (<200 μm). These characteristics, particularly its high surface area and strong water absorption capacity, make it suitable for use as a partial cement replacement in concrete. Prior to use, the biochar was oven-dried for 24 h, ground, and sieved through a 63 μm mesh to ensure uniform particle distribution and optimal dispersion in the cementitious matrix. The natural aggregates were sourced locally and complied with the requirements of BS EN 12620:2013-Aggregates for Concrete [43].

2.2.1. Sieve Analysis-Particle Size Distribution of Biochar and Aggregates

Sieve analysis for biochar, sand, and coarse aggregates was performed per BS EN 933-1 (2012) [44]. Before testing, the samples were oven-dried at 102 °C for 24 h to remove moisture and ensure accurate particle size measurement. The dried samples were then sieved through progressively finer mesh sizes to determine their particle size distribution. The gradation data was used to verify compliance with standard mix design criteria and to achieve consistent workability across different mixes.

2.2.2. Determination of (Specific Gravity) and Water Absorption

The specific gravity and water absorption of biochar and aggregates were determined following BS EN 1097-6 (2022) [45]. Relative density was calculated as the ratio of material density to that of water. Due to biochar's high internal porosity, its water absorption capacity was significantly higher than that of natural aggregates, influencing the water demand and mix design adjustment.

2.3. Mix Design of Concrete

Concrete mixes were designed following the Building Research Establishment (BRE) method, approved by the UK Department of the Environment [46]. Six mix variations were produced, with biochar replacing cement by mass at 0%, 5%, 15%, 30%, 45%, and 60% (Table 3). To isolate the effect of biochar on the fresh and hardened properties of concrete, no chemical or mineral admixtures were included in any mix. The exclusion of admixtures such as superplasticisers ensured that all observed changes in workability, density, and strength were solely attributed to the different biochar replacement levels.

Table 3. Mix design and Partial replacement of cement with biochar.

Mix ID	**1**	**2**	**3**	**4**	**5**	**6**
kg/m^3	**Control Mix (0% Cement Replacement)**	**5% Cement Replacement**	**15% Cement Replacement**	**30% Cement Replacement**	**45% Cement Replacement**	**60% Cement Replacement**
Cement	507	481.7	431.0	354.9	278.9	202.8
Biochar	0	25.4	76.1	152.1	228.2	304.2
Sand	692	692	692	692	692	692
Coarse aggregates	918	918	918	918	918	918
w/c	0.46	0.46	0.46	0.46	0.46	0.46
admixtures	0	0	0	0	0	0

To ensure consistent moisture conditions, all materials were prepared in SSD (saturated surface dry) conditions. Although biochar showed a high-water absorption capacity (217%), it was intentionally used in a dry state without modifying the mixing water. This approach was selected to assess the natural interaction of dry biochar with the cementitious matrix under a constant water–cement ratio of 0.46. Maintaining a fixed w/c ratio enabled direct comparison between mixes and allowed the practical effects of using untreated biochar as a cement replacement to be evaluated. The ground biochar (Figure 1) was manually sieved to maintain a fine, uniform texture suitable for partial cement replacement. Mixing was carried out in a mechanical drum mixer. The dry materials (cement, biochar, sand, and coarse aggregates) were first blended for 1 min, after which water was added gradually and mixing continued for an additional 2–3 min to achieve a uniform consistency. Immediately after mixing, the workability of each batch was assessed using the slump test.

Fresh concrete was then cast into 100 mm × 100 mm cube molds in two layers, with each layer compacted using 25 strokes of a tamping rod and further consolidated on a vibrating table to minimise entrapped air. For each mixed ID, three cube specimens were produced, giving a total of 18 specimens. The molds were covered with plastic sheets to prevent moisture loss during the first 24 h. After demolding at 24 h, all specimens were labelled and placed fully submerged in potable water at 20 ± 2 °C. The cubes were cured for 28 days prior to testing to ensure consistent hydration conditions.

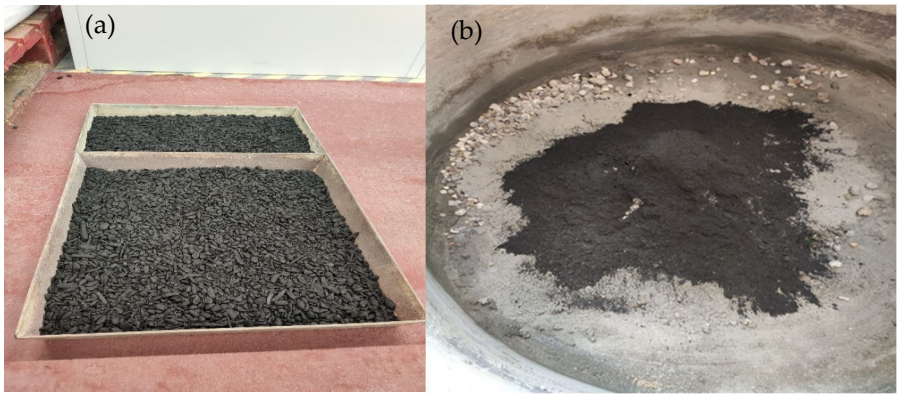

Figure 1. (**a**) Biochar and (**b**) ground biochar in the mix.

2.4. Fresh Concrete Properties

Fresh concrete properties, such as workability and setting time, were evaluated using the slump test and setting time measurements.

2.4.1. Slump Test

The consistency of the concrete mixes was determined using the slump test, following the guidelines of BS EN 12350-2 (2009) [47]. The standard specifies acceptable slump values based on the type of concrete, typically ranging from 10 to 150 mm. The control mix exhibited a slump of 55 mm, while the biochar-incorporated concrete for mix ID 6 showed a reduced slump of 26 mm, indicating lower workability.

2.4.2. Initial Setting and Final Setting Time

Following the procedure specified in BS EN 196-3 (2016) [48], the initial setting time of the cement was determined using a Vicat apparatus. The mortar composition was adjusted to incorporate varying amounts of biochar for different mix IDs, along with a control mix without biochar. The initial setting time was defined as the period required for the mortar to achieve the specified penetration resistance, which typically ranges between 45 and 375 min. The final setting time was determined in accordance with BS EN 196-3 (2011) [49] using the Vicat apparatus equipped with the standard final-setting needle (1 mm^2 cross-sectional area with a 5 mm annular ring). This value represents the time at which the needle fails to penetrate the mortar surface by more than 0.5 mm, indicating that the paste has attained the necessary stiffness. According to the standard, the final setting time should lie between 60 and 600 min.

2.5. Hardened Concrete Properties

2.5.1. Compressive Strength Test

The compressive strength of concrete was determined using 100 mm × 100 mm × 100 mm cube specimens in accordance with BS EN 12390-3 (2019) [50]. Testing was performed on a Universal Testing Machine (UTM). A total of 18 cubes, including control samples, were cast and cured under water for 28 days before testing to evaluate their strength.

2.5.2. Density

Concrete density is defined as the mass per unit volume and typically ranges from 2300 to 2500 kg/m^3, depending on aggregate type, water–cement ratio, admixtures, and cementitious materials. The theoretical wet density of the C40 control mix in this study was 2350 kg/m^3. The density of hardened concrete was determined in accordance with BS EN 12350-6 (2019) [51]. Standard cube specimens of dimensions 100 mm × 100 mm × 100 mm were prepared and cured for 28 days. After curing, the specimens were oven-dried for 24 h

to remove surface moisture and allowed to cool to room temperature. The mass of each specimen was recorded using a calibrated digital balance, and the volume was calculated from the measured cube dimensions.

2.6. The Carbon Footprint of Concrete

The embodied carbon for life cycle stages A1–A3 was calculated for each mix using carbon factors corresponding to the constituent materials. The contribution of each ingredient was determined by multiplying its weight by the respective carbon factors. Two cases were considered: (i) calculation of embodied carbon without accounting for biochar's carbon offsets, and (ii) calculation including biochar's carbon sequestration potential. The certified carbon offset of the biochar used was 2.42 kg CO_2e/kg, reflecting its ability to reduce net emissions, consistent with previous findings on carbon-negative concrete [39]. The main objective of this analysis was to evaluate and compare the carbon footprint of biochar-modified mixes against the control mix.

3. Results and Discussion

3.1. Particle Size Distribution (PSD)

The fine aggregate used in this study was a washed natural sand with a nominal particle size of 2–4 mm, a typical moisture content of 7–8%, and a bulk density of approximately 1450–1650 kg/m^3. Particle size distribution (PSD) analysis showed a uniform gradation, with most sand particles retained on the 0.3 mm sieve (as depicted in Figure 2). The coarse aggregate was a single-sized natural gravel with a nominal size of about 10 mm, comprising predominantly 4–10 mm particles and a typical moisture content of around 3%. The material met common construction-grade quality limits, including shell content below 10%, chloride content below 0.01%, and acid-soluble sulphate content below 0.8%. PSD measurements confirmed that most coarse aggregate particles were within the 7–14 mm range, consistent with a nominal 10 mm aggregate. The raw biochar batch ranged from 63 µm to 7 mm and exhibited a non-uniform gradation due to the wide variation in particle sizes. Only biochar particles passing through a 63 µm sieve were used in the concrete mixes. Sand showed a uniform gradation, with most particles retained on the 0.3 mm sieve. For coarse aggregates, most particles ranged from 7.1 to 14 mm, with very few below 4 mm, and the maximum retention occurred on the 7.1 mm sieve.

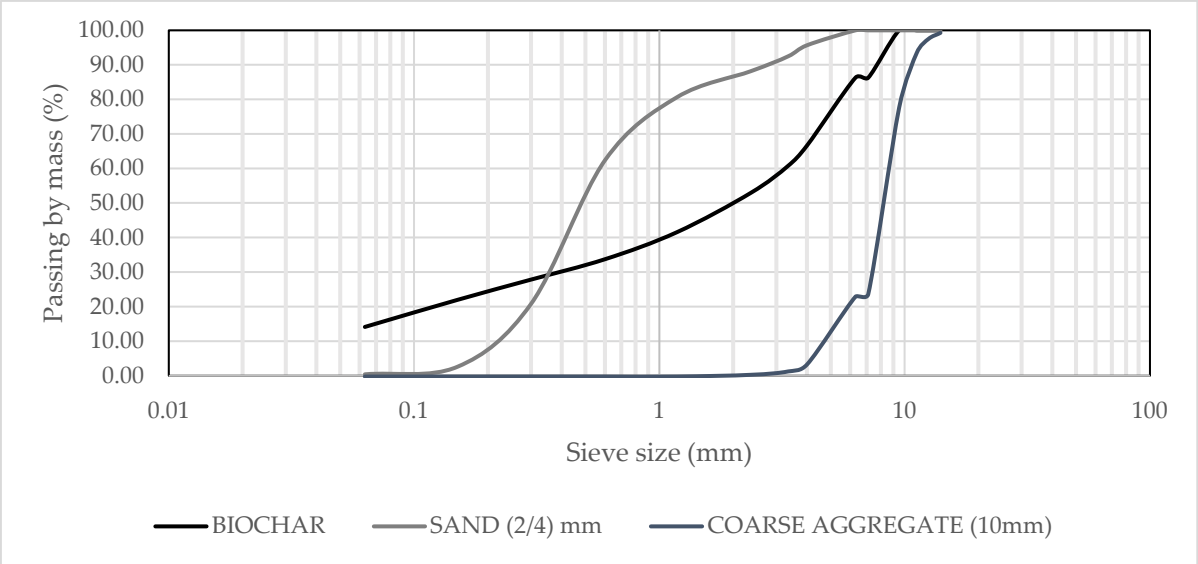

Figure 2. Particle size distribution curve.

3.2. Relative Density (Specific Gravity) and Water Absorption Value

The relative density and water absorption of biochar were determined using a pycnometer test. Biochar exhibited a high 24 h water absorption capacity of 217%, reflecting its strong hygroscopic nature. Its specific gravity was measured as 0.53, indicating a very light material that floats on water.

3.3. Slump Test (Consistency of Concrete)

The slump test was conducted to evaluate the workability of the control mix (0% biochar) and five biochar-modified mixes (Figure 3). The results show that incorporating biochar reduced workability, with the slump decreasing as the biochar content increased. The control mix had a slump of 55.0 mm, whereas Mix ID-6 (60% cement replacement with biochar) recorded a slump of 26.0 mm, a 52.7% reduction. This reduction is attributed to biochar's high-water absorption, which reduces the effective water available in the mix. No admixtures were used in this experiment.

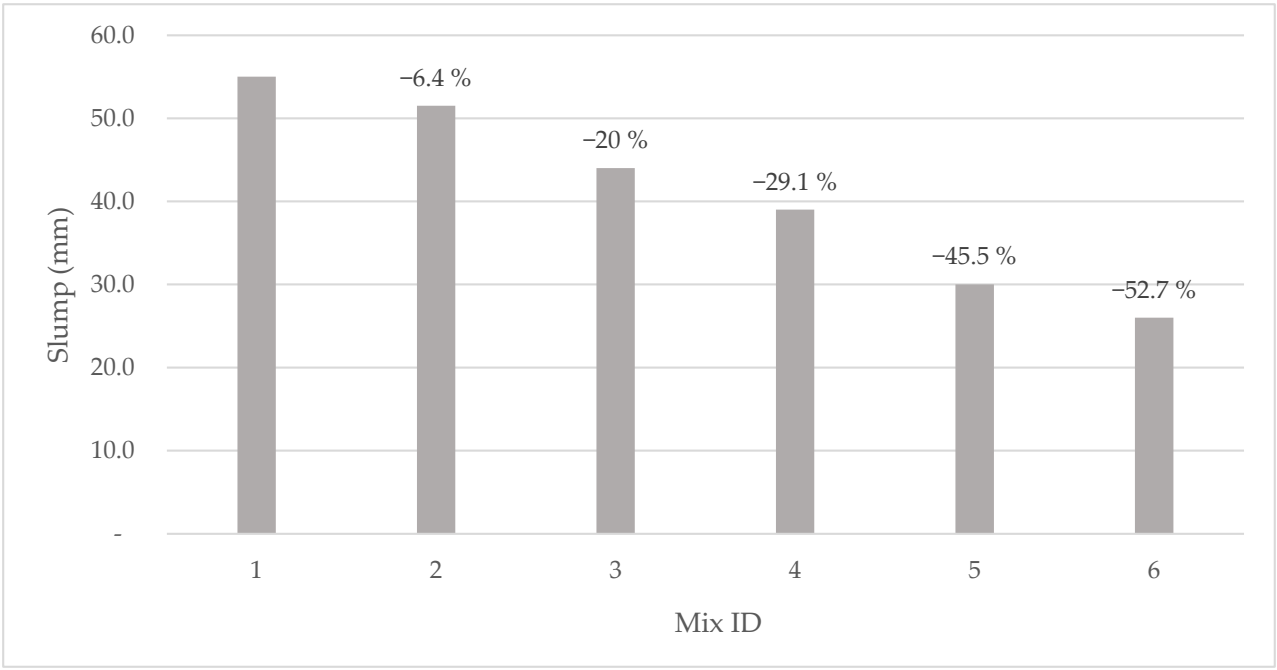

Figure 3. Comparison of slump test results for different concrete mixes, showing the reduction percentage relative to the control mix.

3.4. Initial Setting and Final Setting Time

The initial and final setting times of the control cement paste and biochar-modified pastes were measured, and the results are shown in Figures 4 and 5. The incorporation of biochar significantly reduced both setting times, with the effect more pronounced on the initial setting time due to a reduction in free water content. For 60% cement replacement with biochar, the initial and final setting times decreased by 64% and 13.41%, respectively, compared with the control. At 5% replacement, reductions were 22.67% and 3.66%, respectively, indicating that low biochar additions of less than 5% have minimal impact on setting behavior.

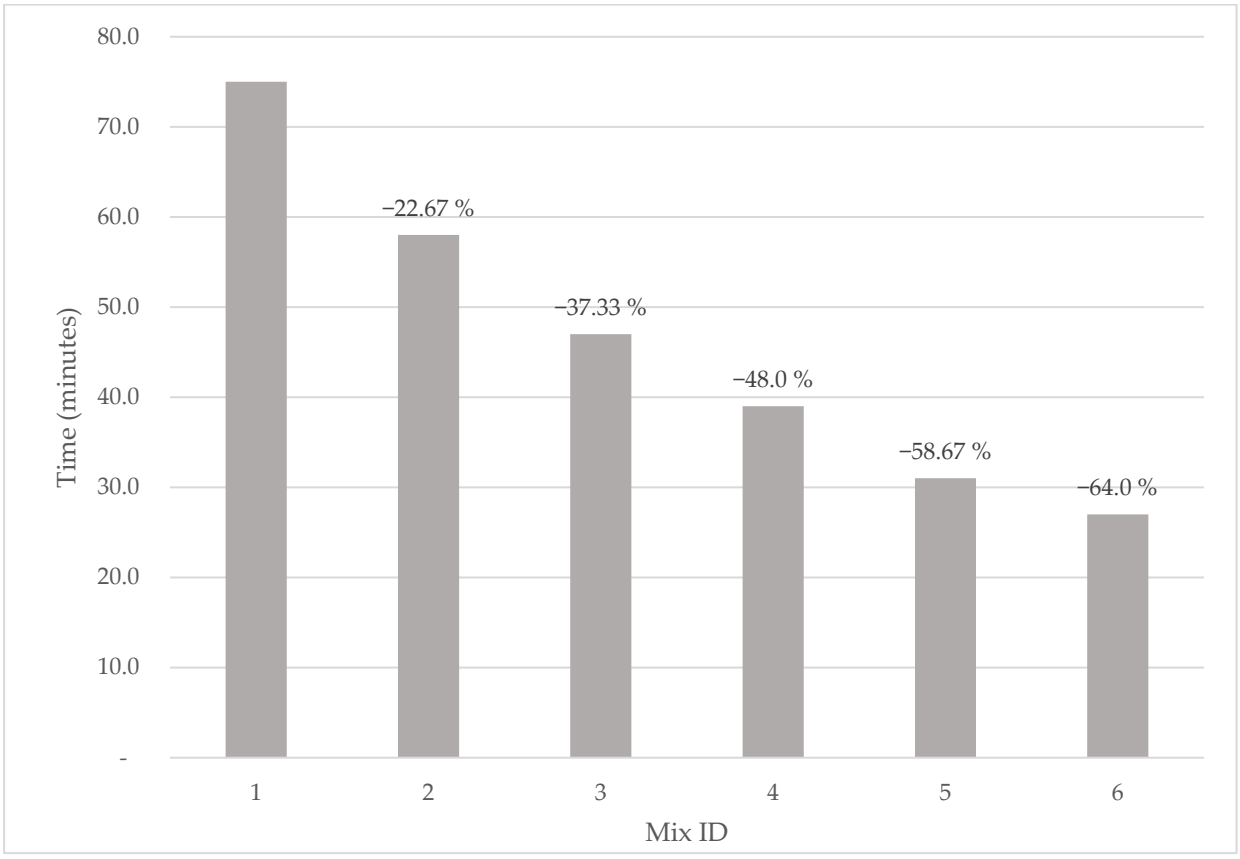

Figure 4. Comparison of initial setting times for various concrete mixes relative to the control mix, showing the reduction percentage.

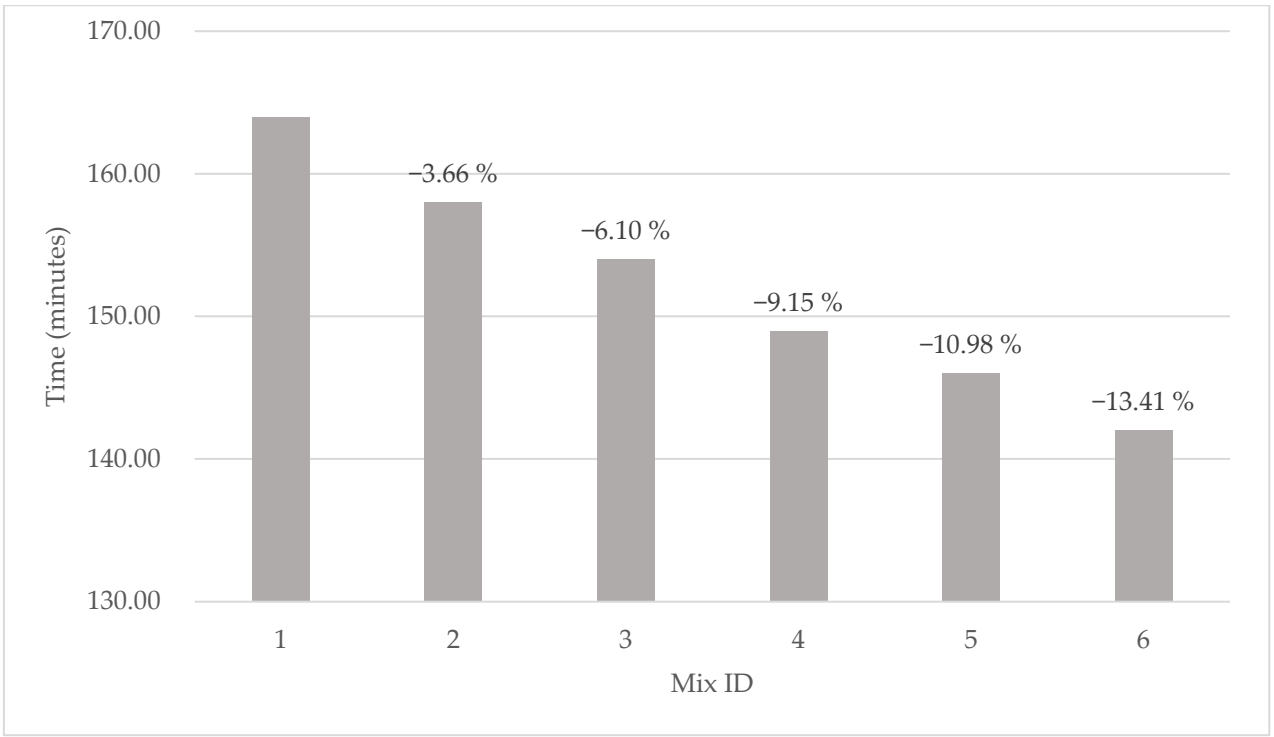

Figure 5. Comparison of final setting times for various concrete mixes relative to the control mix, showing the reduction percentage.

3.5. Compressive Strength

Concrete cubes were tested for compressive strength after 28 days of curing, and the results are presented in Figure 6. The target strength for C40 concrete in this study was 40 N/mm^2. The control mix (0% biochar) achieved an average compressive strength of 41.24 N/mm^2. Compressive strength decreased by increasing biochar content, with reductions of 38.13% for 5% cement replacement and 90.68% for 60% replacement.

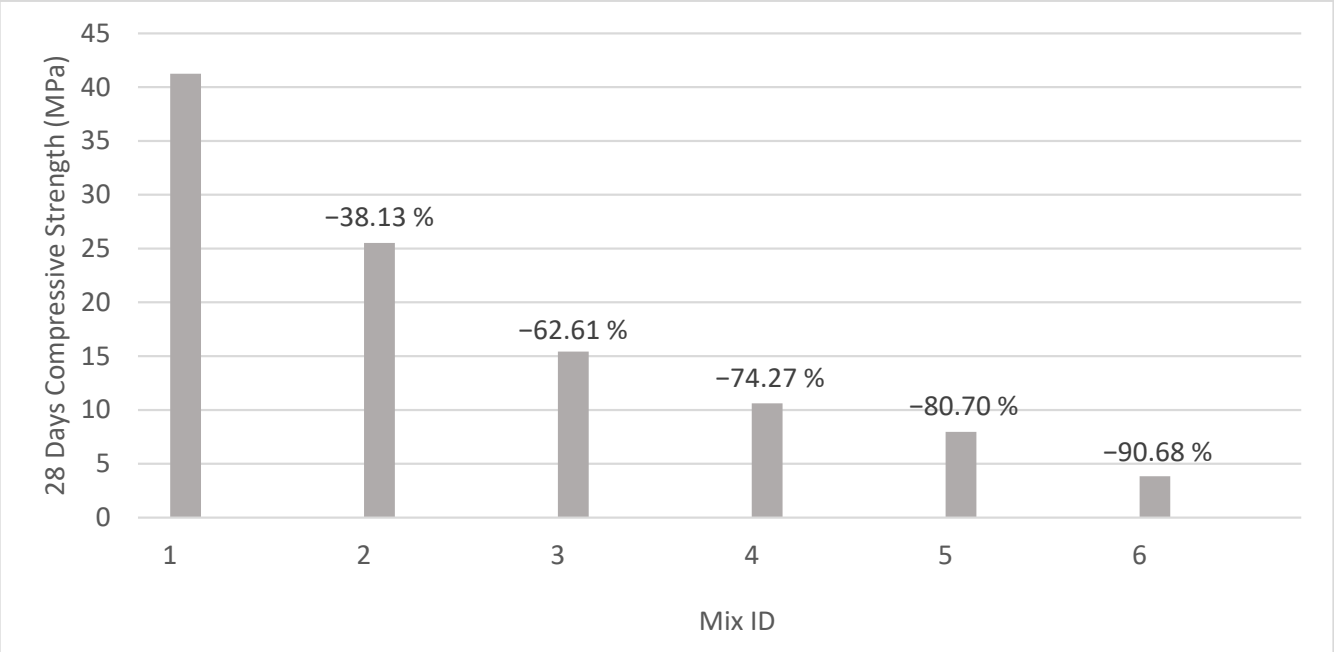

Figure 6. Comparison of compressive strengths for various concrete mixes relative to the control mix, showing the reduction percentage.

The reduction in compressive strength with increasing biochar content can be attributed to several interacting mechanisms. The porous, lightweight nature of biochar increases overall matrix porosity, which reduces the effective load-bearing capacity of the composite. In addition, due to biochar's high water absorption capacity, its incorporation in dry form likely reduced the effective water available for cement hydration, especially at higher replacement levels. Limited hydration restricts the formation of strength-contributing products such as C–S–H gel, resulting in weak interfacial bonding and premature cracking under load. These effects become more pronounced as biochar content increases, explaining the sharp decline in strength observed beyond 5 wt.% replacement. Consequently, although low biochar contents retain partial structural integrity, higher levels render the concrete unsuitable for structural applications. Therefore, the practical use of biochar-modified concrete should be restricted to non-structural or low-load-bearing elements, where sustainability benefits may outweigh mechanical performance losses. Cube failure patterns were observed according to BS EN 12390-3 [50], and all mixes exhibited unsatisfactory failure patterns, as shown in Figure 7.

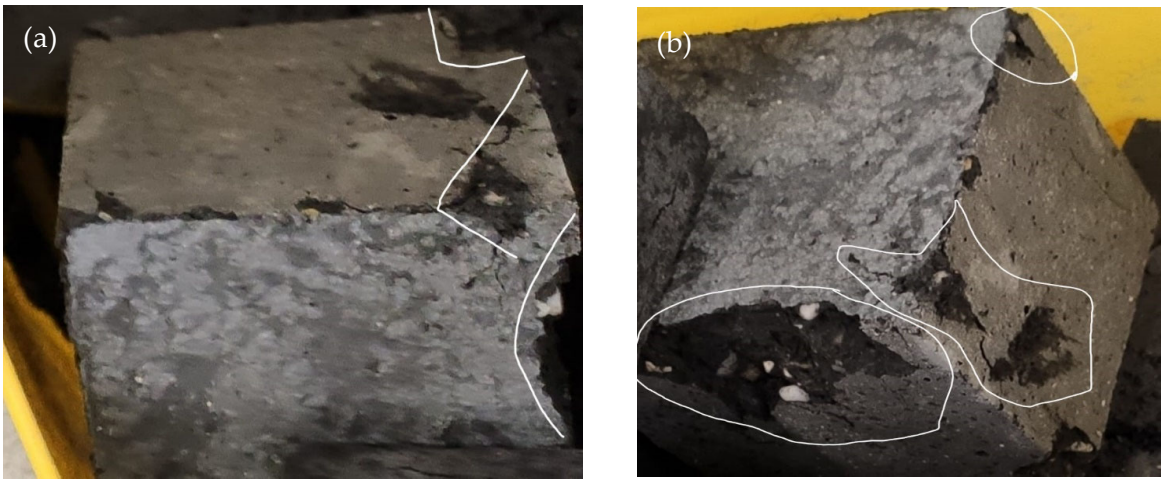

Figure 7. Failure patterns of concrete cubes: (**a**) unsatisfactory failure type 4, and (**b**) unsatisfactory failure type 7.

3.6. Density

The dry density of concrete cubes was calculated from their mass and standard volume (100 mm × 100 mm × 100 mm), with results presented in Figure 8. The control mix exhibited an average density of 2478.7 kg/m^3. Incorporating biochar led to a gradual reduction in density: 5% replacement caused a minor decrease of 1%, 15% replacement reduced density by 6.4%, and 30%, 45%, and 60% replacements resulted in decreases of 9.1%, 14.8%, and 17.3%, respectively. Overall, increasing the proportion of cement replaced by biochar consistently reduced the concrete's dry density.

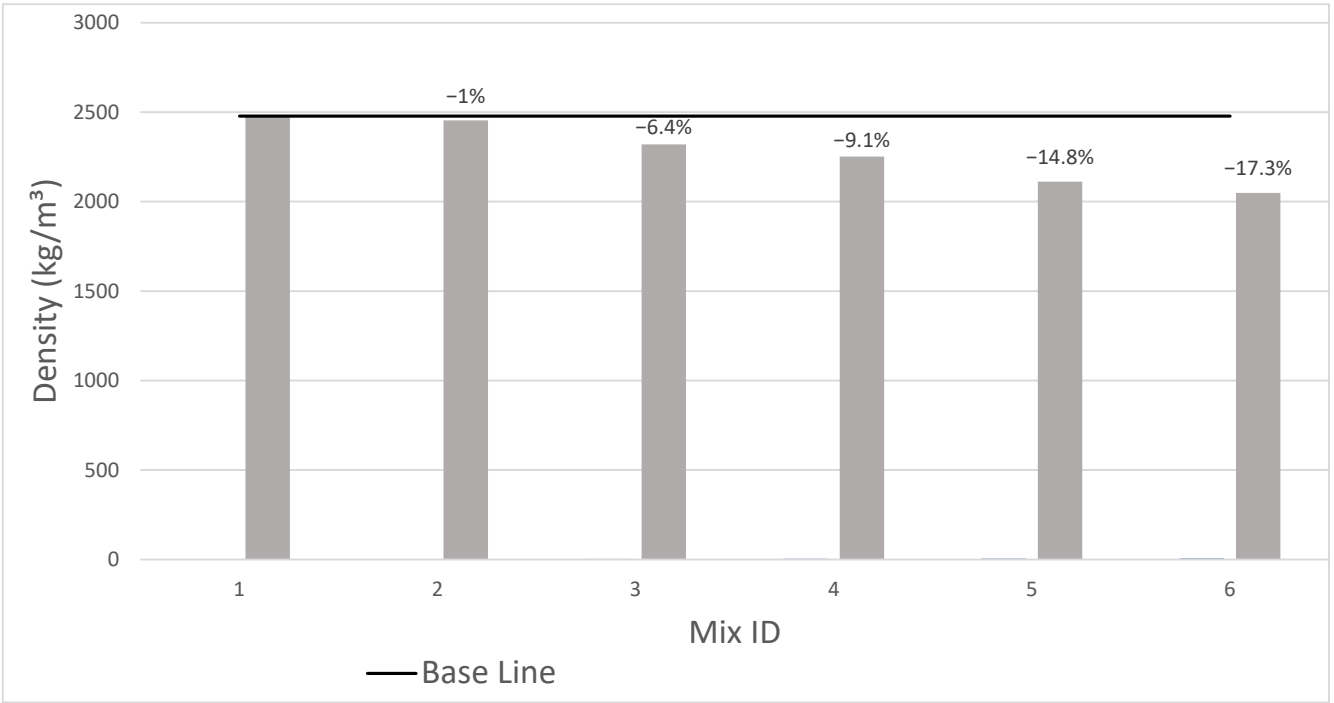

Figure 8. Comparison of dry densities for the control mix and biochar-modified mixes, showing the reduction percentage.

3.7. Carbon Footprint of Concrete

The embodied carbon of the control and biochar-modified concrete mixes was calculated, defined as the total CO_2 equivalent (kg CO_2e) produced to manufacture the constituent materials [52–54]. For analysis, two scenarios were considered:

Case I: Embodied carbon calculated without accounting for biochar's carbon offset. In this case, reductions in cement content directly decreased embodied carbon. Compared with the control mix, cement replacements of 5%, 15%, 30%, 45%, and 60% reduced embodied carbon by 4.9%, 14.7%, 29.4%, 44.1%, and 58.8%, respectively, showing a clear decreasing trend (Figure 9).

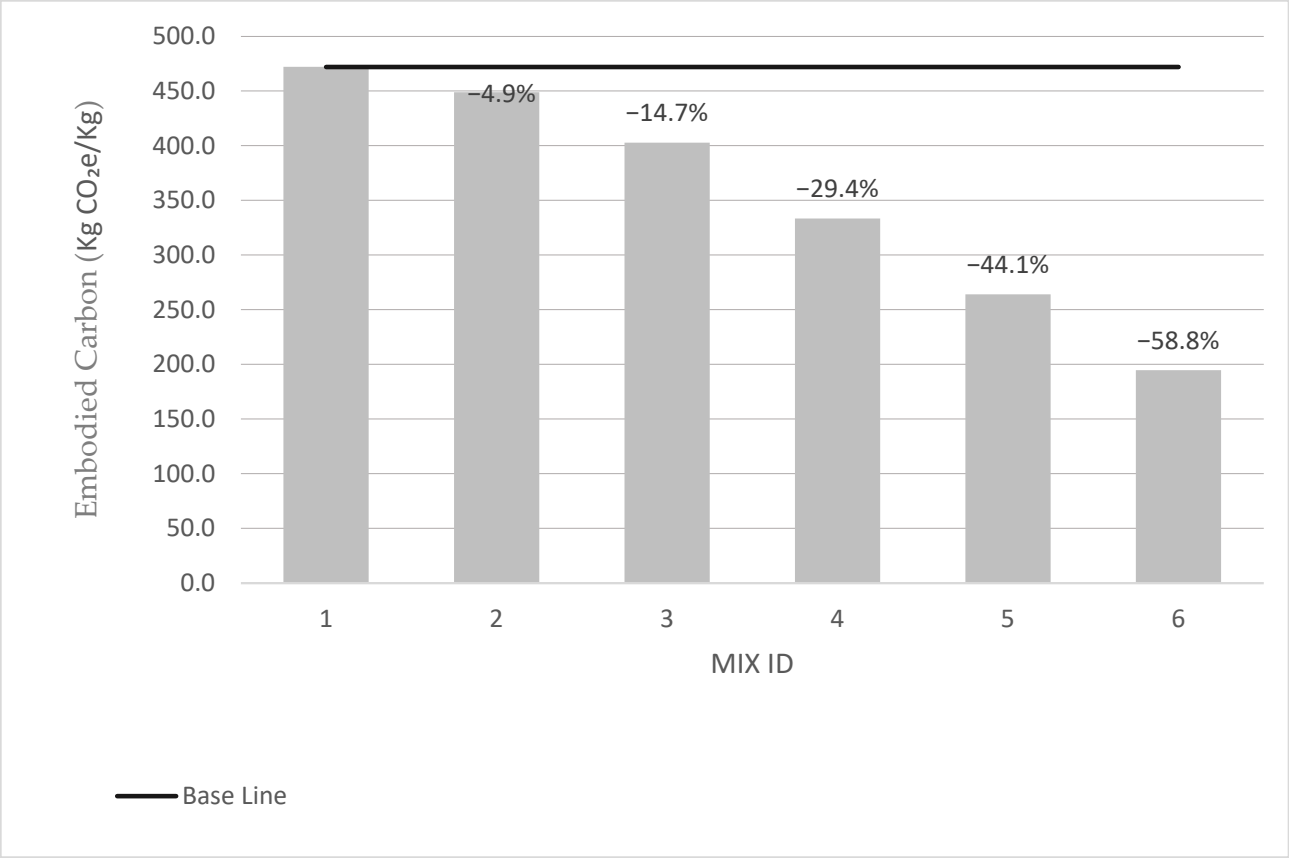

Figure 9. Embodied carbon of concrete mixes compared with the control mix (Mix ID 1), showing reductions in kg CO_2e/Kg.

Case II: Embodied carbon calculated, including biochar's carbon offset, reflecting its carbon sequestration potential. In this scenario, mixes with 30%, 45%, and 60% cement replacement became carbon-negative, while 5% and 15% replacements showed significant reductions in embodied carbon. These results align with previous findings on carbon-negative concrete (Figure 10) [39].

Overall, partial replacement of cement with biochar substantially reduces the carbon footprint, and higher replacement levels can produce carbon-negative concrete due to biochar's sequestration effect.

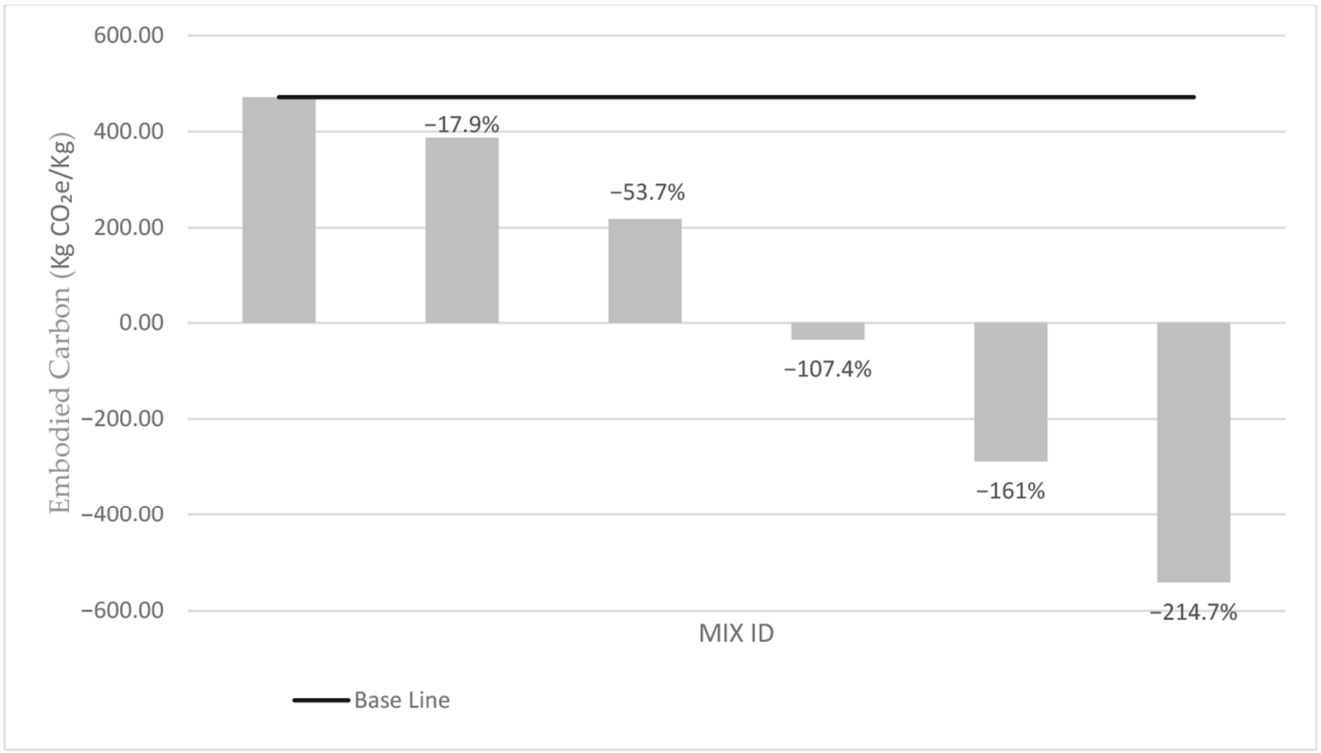

Figure 10. Embodied carbon of concrete mixes compared with the control mix (Mix ID 1), including biochar carbon offsets, showing reductions in Kg CO_2e/Kg.

4. Conclusions

This experimental investigation examined the performance of low-carbon concrete incorporating biochar as a partial replacement for cement. The study evaluated the material's fresh and hardened properties, including setting time, slump, compressive strength, density, and embodied carbon. The following key findings were drawn:

- Setting time: The incorporation of biochar accelerated the setting process. When cement was replaced with 60% biochar, the initial and final setting times decreased by 64% and 13.4%, respectively, compared to the control mix. At lower replacement levels (e.g., 5%), the variation was relatively minor, indicating that small additions (<5%) have a limited impact on workability time.
- Workability (Slump): Increasing biochar content led to a consistent reduction in slump value, with a 6.2% drop at 5% replacement and up to 52.7% at 60% replacement. This reduction is attributed to biochar's high porosity and strong water absorption capacity, which reduces available mixing water.
- Compressive strength: A progressive decline in compressive strength was observed with increasing biochar content, with reductions of 38% at 5% and up to 90% at 60% replacement. The high-water absorption of biochar and its inert nature contribute to this loss of strength. Hence, higher replacement levels are not suitable for structural applications.
- Density: The density of concrete decreased proportionally with biochar addition due to the low specific gravity of biochar. A reduction ranging from 1% (at 5%) to 17.3% (at 60%) was observed.
- Embodied carbon: A significant reduction in embodied carbon was achieved, reaching up to 58.8% at 60% replacement (without accounting for carbon sequestration). When biochar's carbon offset value was considered, mixes containing $\geq$ 30% biochar demonstrated a net carbon-negative footprint.

In summary, the incorporation of biochar in concrete offers a clear trade-off between mechanical performance and environmental benefit. At lower dosages (<5%), biochar can reduce embodied carbon while maintaining acceptable strength, setting time, and density. However, higher substitution levels, while environmentally advantageous, result in substantial strength loss and are therefore more suitable for low-strength and non-structural applications such as masonry blocks, paving units, or lightweight partition materials.

This study contributes to the growing body of knowledge on carbon-neutral construction materials by quantifying the dual effect of biochar on performance and carbon footprint. Future studies should focus on optimising particle size, pre-treatment, and admixture compatibility to achieve a balance between strength and sustainability outcomes.

5. Recommendations for Further Studies

Based on the experimental investigation, results, and conclusion, the following things will be recommended for further investigation:

- Based on the physical characteristics of the hardwood biochar used in this study (high porosity, fine particle size, and low density), it is unlikely to be suitable as a partial replacement for coarse aggregates in structural concrete, which require materials with substantially higher strength and density.
- Biochar's high-water absorption (217% in 24 h) reduces mix workability; hence, it should be used in a saturated surface dry (SSD) condition or with suitable admixtures.
- Dry grinding of the oven-dried biochar produced significant airborne dust during preparation. Wet grinding, followed by re-drying, is therefore recommended to reduce dust emissions and improve handling safety.
- Due to its low specific gravity, biochar tends to segregate during vibration; therefore, gentle compaction methods should be adopted.
- Further studies should include standardized carbon absorption tests to validate biochar's CO_2 sequestration capacity and establish quantitative models for embodied carbon reduction.

Author Contributions: Conceptualization, A.A.A.; Methodology, A.A.A.; Validation, S.J.T.; Formal analysis, S.J.T.; Investigation, S.J.T.; Resources, A.A.A.; Data curation, S.J.T.; Writing—original draft, S.J.T.; Writing—review & editing, A.A.A.; Supervision, A.A.A.; Project administration, A.A.A. All authors have read and agreed to the published version of the manuscript.

Funding: This research received no external funding.

Institutional Review Board Statement: Not applicable.

Informed Consent Statement: Not applicable.

Data Availability Statement: The original contributions presented in this study are included in the article. Further inquiries can be directed to the corresponding author.

Conflicts of Interest: The authors declare no conflicts of interest.

References

1. Moon, D.H.; Park, S.S.; Kang, S.-P.; Lee, W.; Park, K.T.; Chun, D.H.; Rhim, G.B.; Hwang, S.-M.; Youn, M.H.; Jeong, S.K. Determination of kinetic factors of CO_2 mineralization reaction for reducing CO_2 emissions in cement industry and verification using CFD modelling. *Chem. Eng. J.* **2021**, *420*, 129420. [CrossRef]
2. Department for Business, Energy & Industrial Strategy. UK's Path to Net Zero Set Out in Landmark Strategy. GOV.UK, 19 October 2021. Available online: https://www.gov.uk/government/news/uks-path-to-net-zero-set-out-in-landmark-strategy (accessed on 19 February 2024).
3. Zhang, Y.; He, M.; Wang, L.; Yan, J.; Ma, B.; Zhu, X.; Ok, Y.S.; Mechtcherine, V.; Tsang, D.C.W. Biochar as construction materials for achieving carbon neutrality. *Biochar* **2022**, *4*, 59. [CrossRef]

4. Major, J.; Steiner, C.; Downie, A.; Lehmann, J. Biochar effects on nutrient leaching. In *Biochar for Environmental Management: Science and Technology*; Lehmann, J., Joseph, S., Eds.; Earthscan: London, UK; Routledge: London, UK, 2009; pp. 271–287. [CrossRef]
5. Bridgwater, A.V. *Chapter 7. Fast Pyrolysis of Biomass for Energy and Fuels*; RSC Energy and Environment Series; Royal Society of Chemistry (RSC) Publishing: Cambridge, UK, 2010; pp. 146–191. [CrossRef]
6. Bridgwater, A.V. Review of fast pyrolysis of biomass and product upgrading. *Biomass Bioenergy* **2012**, *38*, 68–94. [CrossRef]
7. Downie, A.; Crosky, A.; Munroe, P. Physical Properties of Biochar. In *Biochar for Environmental Management: Science and Technology*; Lehmann, J., Joseph, S., Eds.; Earthscan: London, UK, 2009; pp. 13–32.
8. Lua, A.C.; Yang, T.; Guo, J. Effects of pyrolysis conditions on the properties of activated carbons prepared from pistachio-nut shells. *J. Anal. Appl. Pyrolysis* **2004**, *72*, 279–287. [CrossRef]
9. Ghani, W.A.W.A.K.; Mohd, A.; da Silva, G.; Bachmann, R.T.; Taufiq-Yap, Y.H.; Rashid, U.; Al-Muhtaseb, A.H. Biochar production from waste rubber-wood-sawdust and its potential use in C sequestration: Chemical and physical characterization. *Ind. Crop. Prod.* **2013**, *44*, 18–24. [CrossRef]
10. Gupta, S.; Kua, H.W.; Pang, S.D. Biochar-mortar composite: Manufacturing, evaluation of physical properties and economic viability. *Constr. Build. Mater.* **2018**, *167*, 874–889. [CrossRef]
11. Akhtar, A.; Sarmah, A.K. Novel biochar-concrete composites: Manufacturing, characterization and evaluation of the mechanical properties. *Sci. Total Environ.* **2018**, *616–617*, 408–416. [CrossRef]
12. Gupta, S.; Kua, H.W.; Cynthia, S.Y.T. Use of biochar-coated polypropylene fibres for carbon sequestration and physical improvement of mortar. *Cem. Concr. Compos.* **2017**, *83*, 171–187. [CrossRef]
13. Berodier, E.; Scrivener, K. Understanding the filler effect on the nucleation and growth of C-S-H. *J. Am. Ceram. Soc.* **2014**, *97*, 3764–3773. [CrossRef]
14. Zeidabadi, Z.A.; Bakhtiari, S.; Abbaslou, H.; Ghanizadeh, A.R. Synthesis, characterization and evaluation of biochar from agricultural waste biomass for use in building materials. *Constr. Build. Mater.* **2018**, *181*, 301–308. [CrossRef]
15. Lawrence, P.; Cyr, M.; Ringot, E. Mineral admixtures in mortars. *Cem. Concr. Res.* **2003**, *33*, 1939–1947. [CrossRef]
16. Scrivener, K.L.; Crumbie, A.K.; Laugesen, P. The interfacial Transition Zone (ITZ) between cement paste and aggregate in concrete. *Interface Sci.* **2004**, *12*, 411–421. [CrossRef]
17. Vargas, P.; Restrepo-Baena, O.; Tobón, J.I. Microstructural analysis of interfacial transition zone (ITZ) and its impact on the compressive strength of lightweight concretes. *Constr. Build. Mater.* **2017**, *137*, 381–389. [CrossRef]
18. Mrad, R.; Chehab, G. Mechanical and Microstructure Properties of Biochar-Based Mortar: An Internal Curing Agent for PCC. *Sustainability* **2019**, *11*, 2491. [CrossRef]
19. Dixit, A.; Gupta, S.; Pang, S.D.; Kua, H.W. Waste Valorization using biochar for cement replacement and internal curing in ultra-high performance concrete. *J. Clean. Prod.* **2019**, *238*, 117876. [CrossRef]
20. Gupta, S.; Kua, H.W. Carbonaceous micro-filler for cement: Effect of particle size and dosage of biochar on fresh and hardened properties of cement mortar. *Sci. Total. Environ.* **2019**, *662*, 952–962. [CrossRef]
21. Khushnood, R.A.; Ahmad, S.; Restuccia, L.; Spoto, C.; Jagdale, P.; Tulliani, J.-M.; Ferro, G.A. Carbonized nano/microparticles for enhanced mechanical properties and electromagnetic interference shielding of cementitious materials. *Front. Struct. Civ. Eng.* **2016**, *10*, 209–213. [CrossRef]
22. Restuccia, L.; Ferro, G.A. Promising low cost carbon-based materials to improve strength and toughness in cement composites. *Constr. Build. Mater.* **2016**, *126*, 1034–1043. [CrossRef]
23. Qin, Y.; Pang, X.; Tan, K.; Bao, T. Evaluation of pervious concrete performance with pulverized biochar as cement replacement. *Cem. Concr. Compos.* **2021**, *119*, 104022. [CrossRef]
24. Zhang, L.; Jiang, J.; Holm, N.; Chen, F. Mini-chunk biochar supercapacitors. *J. Appl. Electrochem.* **2014**, *44*, 1145–1151. [CrossRef]
25. Zhang, M.-H.; Li, H. Pore structure and chloride permeability of concrete containing nano-particles for pavement. *Constr. Build. Mater.* **2011**, *25*, 608–616. [CrossRef]
26. Jiang, J.; Zhang, L.; Wang, X.; Holm, N.; Rajagopalan, K.; Chen, F.; Ma, S. Highly ordered microporous woody biochar with ultra-high carbon content as supercapacitor electrodes. *Electrochimica Acta* **2013**, *113*, 481–489. [CrossRef]
27. Singh, B.; Camps-Arbestain, M.; Lehmann, J. Biochar pH, electrical conductivity and liming potential. In *Biochar: A Guide to Analytical Methods*; Singh, B., Camps-Arbestain, M., Lehmann, J., Eds.; CSIRO Publishing: Boca Raton, FL, USA, 2017; pp. 23–38. [CrossRef]
28. Wang, Y.; Shi, Z.; Huang, Y.; Ma, Y.; Wang, C.; Chen, M.; Chen, Y. Supercapacitor devices based on graphene materials. *J. Phys. Chem. C* **2009**, *113*, 13103–13107. [CrossRef]
29. Gabhi, R.S.; Kirk, D.W.; Jia, C.Q. Preliminary investigation of electrical conductivity of monolithic biochar. *Carbon* **2017**, *116*, 435–442. [CrossRef]
30. Lura, P.; Wyrzykowski, M.; Tang, C.; Lehmann, E. Internal curing with lightweight aggregate produced from biomass-derived waste. *Cem. Concr. Res.* **2014**, *59*, 24–33. [CrossRef]

31. Castro, J.; Keiser, L.; Golias, M.; Weiss, J. Absorption and desorption properties of fine lightweight aggregate for application to internally cured concrete mixtures. *Cem. Concr. Compos.* **2011**, *33*, 1001–1008. [CrossRef]
32. Ling, Y.; Wu, X.; Tan, K.; Zou, Z. Effect of Biochar Dosage and Fineness on Concrete Mechanical Properties and Durability of Concrete. *Materials* **2023**, *16*, 2809. [CrossRef]
33. Wang, L.; Chen, L.; Tsang, D.C.; Guo, B.; Yang, J.; Shen, Z.; Hou, D.; Ok, Y.S.; Poon, C.S. Biochar as green additives in cement-based composites with carbon dioxide curing. *J. Clean. Prod.* **2020**, *258*, 120678. [CrossRef]
34. Fang, H.-Y.; Chaney, R.C. *Introduction to Environmental Geo Technology*; CRC Press eBooks; CRC Press: London, UK, 2016. [CrossRef]
35. Bamdad, H.; Hawboldt, K.; MacQuarrie, S.; Papari, S. Application of biochar for acid gas removal: Experimental and statistical analysis using CO_2. *Environ. Sci. Pollut. Res.* **2019**, *26*, 10902–10915. [CrossRef]
36. Creamer, A.E.; Gao, B.; Zhang, M. Carbon dioxide capture using biochar produced from sugarcane bagasse and hickory wood. *Chem. Eng. J.* **2014**, *249*, 174–179. [CrossRef]
37. Dissanayake, P.D.; You, S.; Igalavithana, A.D.; Xia, Y.; Bhatnagar, A.; Gupta, S.; Kua, H.W.; Kim, S.; Kwon, J.-H.; Tsang, D.C.; et al. Biochar-based adsorbents for carbon dioxide capture: A critical review. *Renew. Sustain. Energy Rev.* **2020**, *119*, 109582. [CrossRef]
38. Lahijani, P.; Mohammadi, M.; Mohamed, A.R. Metal incorporated biochar as a potential adsorbent for high capacity CO_2 capture at ambient condition. *J. CO2 Util.* **2018**, *26*, 281–293. [CrossRef]
39. Chen, L.; Zhang, Y.; Wang, L.; Ruan, S.; Chen, J.; Li, H.; Yang, J.; Mechtcherine, V.; Tsang, D.C. Biochar-augmented carbon-negative concrete. *Chem. Eng. J.* **2022**, *431*, 133946. [CrossRef]
40. Lin, X.; Li, W.; Guo, Y.; Dong, W.; Castel, A.; Wang, K. Biochar-cement concrete toward decarbonization and sustainability for construction: Characteristic, performance and perspective. *J. Clean. Prod.* **2023**, *419*, 138219. [CrossRef]
41. Haque, M.I.; Khan, R.I.; Ashraf, W.; Pendse, H. Production of sustainable, low-permeable and self-sensing cementitious composites using biochar. *Sustain. Mater. Technol.* **2021**, *28*, e00279. [CrossRef]
42. European Biochar Foundation (EBC). *European Biochar Certificate—Guidelines for a Sustainable Production of Biochar, Version 10.1*; European Biochar Foundation (EBC): Arbaz, Switzerland, 2022. Available online: https://www.european-biochar.org/en/download (accessed on 26 November 2025).
43. *BS EN 12620:2013*; Aggregates for Concrete. BSI Standards Limited: London, UK, 2013.
44. *BS EN 933-1*; Tests for Geometrical Properties of Aggregates. Part 1: Determination of Particle Size Distribution. Sieving Method. British Standards Institution: London, UK, 2012.
45. *BS EN 1097-6*; Tests for Mechanical and Physical Properties of Aggregates. Part 6: Determination of Particle Density and Water Absorption. British Standards Institution: London, UK, 2022.
46. *Design of Normal Concrete Mixes*, 2nd ed.; Department of the Environment, Building Research Establishment: Garston, UK, 1992.
47. *BS EN 12350-2*; Testing Fresh Concrete. Slump Test. British Standards Institution: London, UK, 2009.
48. *BS EN 196-3*; Methods of Testing Cement. Determination of Setting Times and Soundness. British Standards Institution: London, UK, 2016.
49. *BS EN 197-1:2011*; Cement—Part 1: Composition, Specifications and Conformity Criteria for Common Cements. British Standards Institution: London, UK, 2011.
50. *BS EN 12390-3*; Testing Hardened Concrete. Compressive Strength of Test Specimens. British Standards Institution: London, UK, 2019.
51. *BS EN 12350-6*; Testing Fresh Concrete. Density. British Standards Institution: London, UK, 2019.
52. Gibbons, O.P.; Orr, J.J.; Archer Jones, C.; Arnold, W.; Green, C. *How to Calculate Embodied Carbon*, 2nd ed.; Institution of Structural Engineers (IStructE): London, UK, 2022.
53. Kanavaris, F.; Gibbons, O.; Walport, E.; Shearer, E.; Abbas, A.; Orr, J.; Marsh, B. Reducing embodied carbon dioxide of structural concrete with lightweight aggregate. *Proc. Inst. Civ. Eng.-Eng. Sustain.* **2022**, *175*, 75–83. [CrossRef]
54. Abbas, A.; Mahadevan, M.; Prajapati, S.; Ayati, B.; Kanavaris, F. Development of low-carbon lightweight concrete using pumice as aggregate and cement replacement. In Proceedings of the RILEM International Conference on Synergising Expertise Towards Sustainability and Robustness of Cement-Based Materials and Concrete Structures (SynerCrete'23), Milos, Greece, 14–16 June 2023; Springer: Cham, Switzerland, 2023. [CrossRef]